VETOR

Porosity Measurement in B_4C-Nb Composite Through Digital Image Analysis and Processing☆

Medida de Porosidade em Compósitos B_4C-Nb por Meio de Análise e Processamento Digital de Imagem

Marcos Paulo Dornellas[1,†], Vinicio Coelho da Silva[1], Getúlio da Silva Abreu[2], Geronimo Perez[3], Marcello Filgueira[2], Marília Garcia Diniz[1]

[1]*Universidade do Estado do Rio de Janeiro, Rio de Janeiro, Brasil*
[2]*Universidade Estadual do Norte Fluminense, Campos dos Goytacazes, Brasil*
[3]*Universidade Federal Fluminense, Niterói, Brasil*
[†]**Corresponding author:** marcosp.dornellas@gmail.com

Abstract

Constant research efforts have been conducted in materials selection to combine and improve the properties of interest, service life and production cost. In this context, boron carbide (B_4C) stands out for having a high mechanical performance, being the material that has the fourth-highest hardness (>29 GPa) among ceramic materials. Unfortunately, porosity is seen as a limiting factor for the high performance of this group of materials, to which boron carbide is found. Porosity control is conducted through imprecise techniques, and indirect or costly measures for quantification. This work quantified the porosity of boron-niobium carbide (B_4C-Nb) composites obtained from a high-pressure, high-temperature (HPHT) sintering process through analysis and digital image processing (DIP) by optical microscopy (OM) after surface preparation with controlled and automated parameters. The results obtained were compared with the mercury intrusion porosimetry method. In addition, the composites were imaged by scanning electron microscopy (SEM) and semi-quantitative chemical characterization was performed using the energy dispersive spectroscopy (EDS) technique which confirmed through the weak emitted signals that the points observed by OM are pores.

Keywords

Advanced ceramics • Boron carbide with niobium • Porosity • Digital image processing.

Resumo

Esforços constantes de pesquisa têm sido conduzidos na seleção de materiais com o intuito de combinar e aprimorar as propriedades de interesse, o tempo de vida útil e o custo de produção. Nesse contexto, o carbeto de boro (B_4C) se destaca por possuir um elevado desempenho mecânico, sendo o material que possui a quarta maior dureza (>29 GPa) entre os materiais cerâmicos. Entretanto, a porosidade é vista como fator limitador do alto desempenho desse grupo de materiais, ao qual o B_4C se encontra. O controle da porosidade é usualmente realizado por meio de técnicas imprecisas, de medidas indiretas ou de alto custo para a sua quantificação. Este trabalho objetivou quantificar a porosidade de compósitos de carbeto de boro-nióbio (B_4C-Nb) obtidos por sinterização em alta pressão

☆ This article is an extended version of the work presented at the Joint XXIV ENMC National Meeting on Computational Modelling and XII ECTM Meeting on Science and Technology of Materials, held in webinar mode, from October 13th to 15th, 2021.

– alta temperatura (HPHT- high-pressure, high-temperature) e analisados por processamento digital de imagens (PDI). Essas imagens foram obtidas por microscopia óptica (MO) após preparação da superfície com parâmetros controlados e automatizados. Os resultados da porosidade obtidos por PDI foram comparados com valores de densidade relativa obtidos por método de porosimetria por intrusão de mercúrio. Os compósitos foram observados por microscopia eletrônica de varredura (MEV) e submetidos à análise química semiquantitativa por espectroscopia de dispersão de energia (EDS) que confirmou por meio dos fracos sinais emitidos que os pontos observados por MO são poros.

Palavras-chave

Cerâmicos avançados • Carbeto de boro com nióbio • Porosidade • Processamento digital de imagem

1 Introduction

The search for combining the properties of interest, versatility of use, high durability and low production cost has been the target of constant efforts in research on material selection [1].

In this context, boron carbide (B_4C) has aroused great interest for its structural and functional applications due to its excellent mechanical and physicochemical properties when compared to other ceramics, such as hardness (fourth hardest ceramic), low density (2,52 g/cm^3), high melting point (2450 °C), high modulus of elasticity, good wear and corrosion resistance, and high neutron absorption capacity [1–3].

However, there are still difficulties in sintering and porosity control, which is considered limiting for the production and performance of these materials. There are challenges regarding the sintering of B_4C. Ji et al.[2] claim that B_4C has poor sintering ability and that pure preparation of this ceramic by traditional sintering technologies is almost impossible. Therefore, one way to improve the mechanical properties of B_4C-based composites is to use high-pressure, high-temperature (HPHT) sintering with new binder. Considering that niobium-carbon composites, such as niobium carbide (NbC), are already used in cutting tool compositions, Nb has shown promise as a binder material for obtaining B_4C-Nb composites to be used for this same purpose [3].

The intention of using niobium as an additive is to improve the sintering process. Another justification for the addition of niobium to the boron carbide matrix is the fact that Brazil has the largest world reserve of the metal, in addition to being the largest producer, and thus sufficient to meet the demands of the domestic and foreign market, with interest in finding new applications for this material. [3].

For the evaluation and quantification of porosity in advanced ceramics there are several effective techniques, such as computed tomography, however, these techniques require specific equipment with high acquisition and maintenance values, which led to the search for alternatives that provide equally safe and lower cost results. The use of quantitative stereology measurement techniques and digital image processing (DIP) may be an option [4].

This work aimed to quantify the porosity (volumetric pore fraction, Vv %) of B_4C-Nb composites sintered in HPHT through images obtained by optical microscopy (OM) and digital image processing (DIP).

2 Material and Methods

The B_4C-Nb composites were obtained and provided for this work by Abreu [3] using HPHT by two (2) steps:

The first step consisted in the preparation and characterization of B_4C-Nb mixtures with Nb percentages varying from 2, 5, 10 and 20% by mass. The B_4C and Nb powders were subjected to high energy milling in a SPEX8000 type mill, with the following parameters:

(a) grinding times: 0 h (manual mixing), 2, 5 and 10 h, with 30-minute beats and 15-minute rest/cooling interval;

b) The Process Control Agent was cyclohexane P.A. da marca (Neon®);

c) The material used in the jar and in the grinding spheres of the mill was tungsten carbide (WC);

d) The sphere/powder mass ratio (mixture) was 10:1, that is, to each milling of 2 g of mixture, 20 g of WC spheres were added.

After manufacturing the B_4C-Nb mixtures, it was necessary to characterize the powders to define the best MAE time to sinter the B_4C-Nb powders with different percentages of Nb.

In the second stage, the HPHT type sintering of the B_4C-Nb powders, a 630 tf press was used with the raw materials that were processed with high energy milling and optimal grinding times defined by first step.

The sintering parameters were set at: 7.7 GPa, 1700 °C, 1100 W, 3 min time with the percentages by mass of Nb at: 2, 5, 10 and 20%.

The sintered composites had a relatively regular cylindrical shape, with height (h) and diameter (d) approximately 4 mm x 4 mm, regardless of the Nb [3].

For this work, the sintered samples were embedded in phenolic resin using an Arotec PRE-40Mi embedding machine. After that, four samples of the composite were selected for each mass percentage of Nb (2, 5, 10 and 20%) and were submitted to the grinding and polishing stages with an automatic polisher model PRESI MECATECH 334 and Reflex Concept i-MAX sanding disks. The grinding process was performed with an 18 μm sanding disc and the machine was programmed for 1000 seconds, with a load of 1 N, rotation speed of 60 rpm for the base and 60 rpm for the head in opposite directions, using running water as a lubricant.

After grinding, the polishing process was performed with PRESI MECAPREX cloths of 6 and 1 μm with PRESI MECAPREX diamond suspensions of 6 and 1 μm, subsequently, with a speed of 300 rpm for the base, 150 rpm for the head in opposite directions and load of 0.25 N. 50% distilled water and 48% alcohol was used as lubricant. Table 1 details the polishing conditions used.

Table 1: Parameters used for polishing.

Polishing Step	Polishing Cloth (μm)	Lubricant	Diamond suspension	Rotation of head/base (rpm)	Time (s)	Load (kgf)
1	6	0.85 mL every 10 s	0.25 mL every 100 s	300/150	1200	0.25
2	1	0.85 mL every 10 s	0.25 mL every 100 s	300/150	3300	0.25

However, when the polishing step described in Table 1 was performed on the B_4C sample with an Nb percentage of 20%, the polishing cloth tore near the end of polishing step 1 with about 350 seconds remaining. Still, polishing step 2 was started with a new 1 μm polishing cloth and again tore with approximately 1000 seconds of polishing time elapsed. Thus, the parameters needed to be changed for this specific condition of the composite. Table 2 presents the parameters that made it possible to achieve the goal of obtaining a highly polished surface for the B_4C-Nb composite with 20% Nb.

Table 2: Parameters used in polishing B_4C with 20% by mass Nb.

Polishing Step	Polishing Cloth (μm)	Lubricant	Diamond suspension	Rotation of head/base (rpm)	Time (s)	Load (kgf)
1	6	0.85 mL every 5 s	0.25 mL every 100 s	100/50	1200	0.1
2	1	0.85 mL every 5 s	0.25 mL every 100 s	100/50	3300	0.1

At the end of the grinding and polishing process, a sequence of images of the sample surfaces was collected using a ZEISS Imager 1M optical microscope with a digital capture system. A total of 160 images were obtained, 40 for each type of composite studied, in distinct and non-overlapping regions of the previously prepared surfaces. All images collected for PDI had same original 500x magnification.

The DIP was performed using the program Fiji (It's Just Image J) version 1.53C. All images were processed individually and involved pre-processing, segmentation, and attribute extraction steps. Brightness and contrast adjustment, thresholding segmentation, artifact elimination, and later extraction of the selected attributes were performed. Fig. 1 (a) shows the selected area of the original image for porosity measurement and Fig. 1 (b) shows, after all procedures, the objects of interest whose areas were quantified in relation to the original image (whites). Thus, the pore area Aa (%) or the volume fraction Vv (%) was obtained for each produced composite.

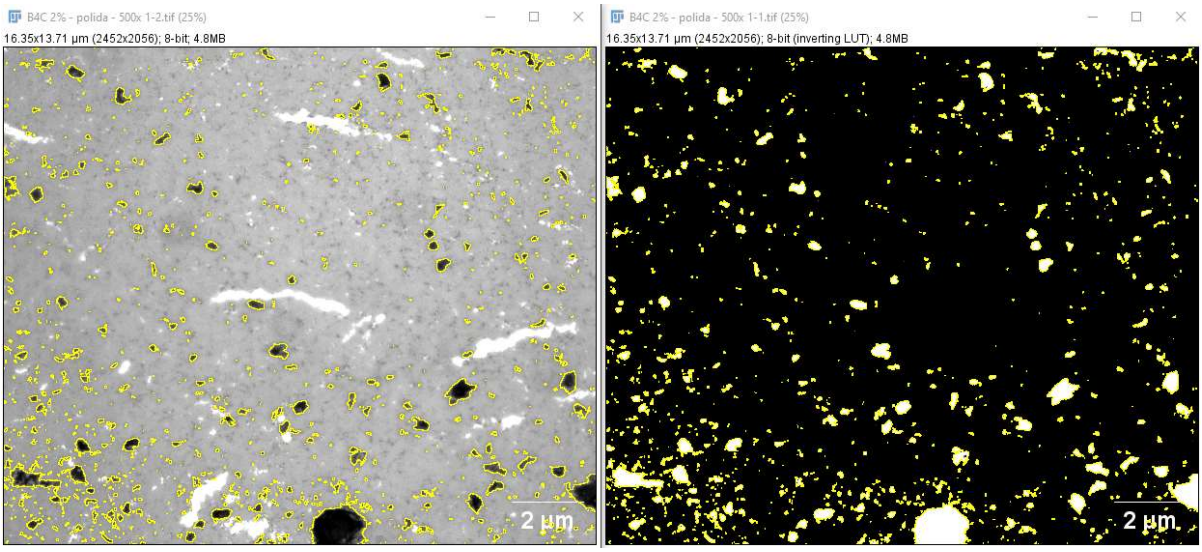

Figure 1: Initial image of the B_4C-Nb sample with 2% Nb containing pores (dark regions) (a) and the result of the area selected for measurement (white regions) (b).

For the same images that were processed to obtain the pore Vv (%) values, the automatic segmentation technique by Stacks was applied, whose the parameters used for the segmentation and separation of objects selected for only one image within a group of images, are applied to all of them simultaneously with the purpose of reducing the processing time. This method segments a set of images [5].

The composites containing 5 and 20% Nb were analyzed by Oxford Instruments Energy Dispersive Spectroscopy (EDS) detector coupled to a JEOL JSM 7100F scanning electron microscope (SEM) with a FEG source operating at 15 kV, for semiquantitative chemical analysis of the chemical elements present and for confirmation of the presence of pores.

3 Results and discussions

The experimental procedure was conducted to obtain quality images of the cross section of the material and to minimize the impacts of imperfection in preparation (scratches, scuffing), giving a finish specular for the surface. The ceramography step used in surface preparation is one of the biggest barriers to obtain adequate images, as well as, for the DIP technique, since ceramic materials have characteristics that hinder this process, unlike metallic materials. [4]. The ideal grinding and polishing parameters were defined only after several qualitative visual tests, which allowed obtaining images of the surfaces without scratches, scuffing and well-polished. Fig. 2 shows the cross section of one of the composites studied, where the sintered material had a background of a gray matrix interspersed with light-colored objects and the presence of pores (dark tones).

All samples had dimensions measured before and after the grinding and polishing steps, to verify the depth reached after the preparation was completed. The samples were thinned out approximately 0.1 mm, a value significantly larger than the highest pore size found within the composites analyzed, thus ensuring that the pores measured were internal and not superficial. Fig. 2 shows the largest pore size found in the MO images.

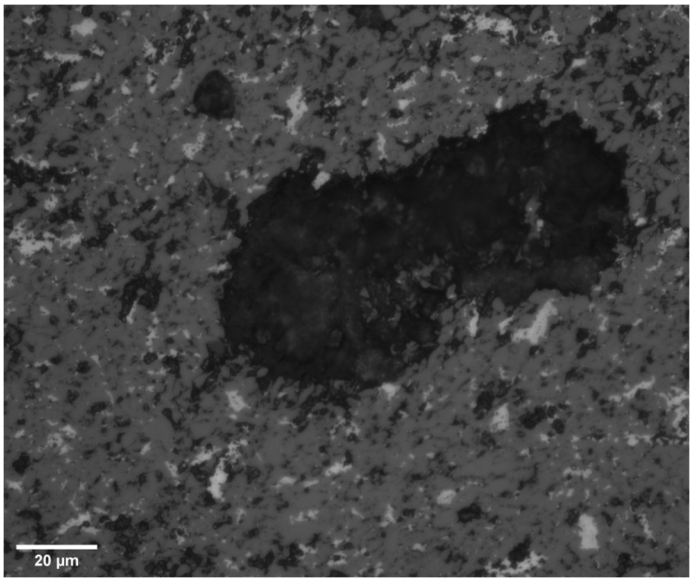

Figure 2: A micropore of 105 µm found in the B_4C sample with 10% Nb at 500x magnification.

The results of the pore quantification obtained from DIP are shown in Table 3:

Table 3: Volumetric fraction Vv percent of pores for the B_4C-Nb composites.

B_4C with 2% Nb		
DIP performed	Average	Standard deviation
manual	7.09%	1.93
stacks	10.61%	2.66
B_4C with 5% Nb		
DIP performed	Average	Standard deviation
manual	13.80%	4.15
stacks	26.61%	23.23
B_4C with 10% Nb		
DIP performed	Average	Standard deviation
manual	24.87%	10.58
stacks	27.14%	11.24
B_4C with 20% Nb		
DIP performed	Average	Standard deviation
manual	20.79%	7.51
stacks	34.63%	19.45

Analyzing the coefficients of variation, the results obtained using both methods were close, except for the images of composites with 5% and 20% Nb. These differences occurred due to variations in luminosity and brightness during the capture of images for these two groups only, which strongly affected the results obtained using the segmentation method by the group of images (stacks). The method of quantification by stacks allows a large reduction in image processing time, which in this work was 60% in relation to the manual method, in which images are processed individually. However, the reliability of the results obtained with the fast method using stacks is only possible when all the images processed in that group present similar characteristics for the segmentation step.

Fig. 3 exemplifies the differences in contrast and brightness for images obtained for the same composite from the group with 5% Nb. These differences make the method by stacks impossible, and the results obtained reinforce the need to obtain images with the same similarity parameters, such as brightness and lighting, to facilitate the PDI.

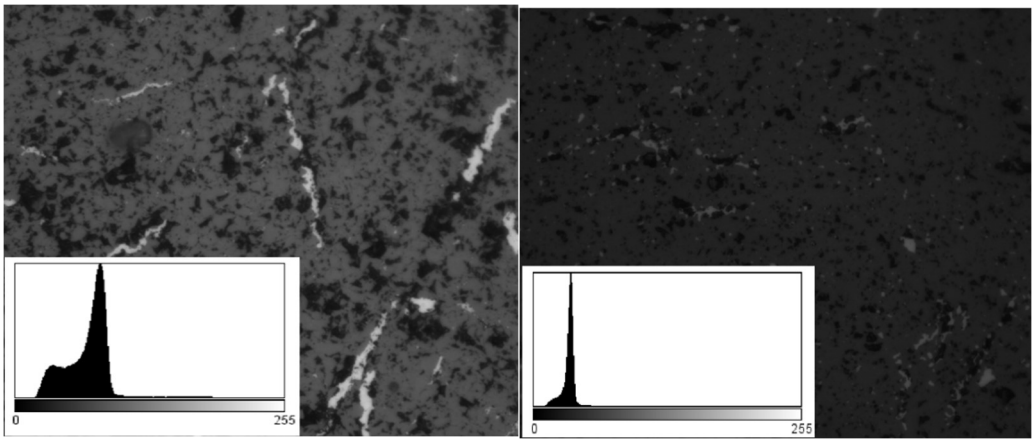

Figure 3: Example of the contrast of the images obtained by MO of the B_4C samples with 5% Nb and 500x magnification. The histogram (frequency of number of pixels from 0 -1 *versus* shade of gray from 0 - 255) on the left shows the concentration of hues in the middle part of the scale.

The use of the technique of DIP stacks for the analysis of ceramics is common in the literature [6-8] when the images have similar characteristics. However, this does not always occur, particularly when the images are acquired in different microscopes, by different operators, lighting systems with different settings or even for samples with different flatness.

Fig. 4 and Table 4 show the results obtained using SEM and EDS for the analyzed composites. They mainly presented a gray matrix based on boron, particles, and veins of lighter tones (phases of higher atomic mass and based on Nb, W and Fe) and pores. The presence of W and Fe are probably associated with the milling process that used WC jar and spheres, containing some Fe as a contaminant. SEM and EDS analyses confirmed that the dark toned regions observed in the MO images were essentially pores.

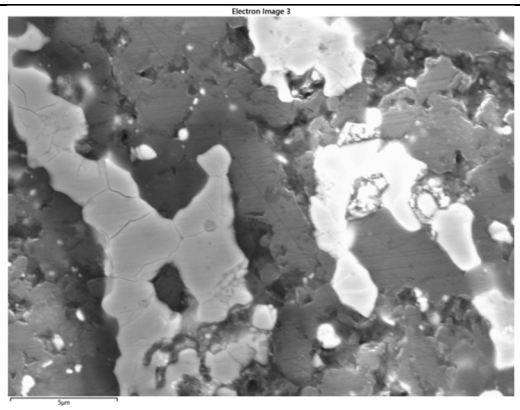

(a)

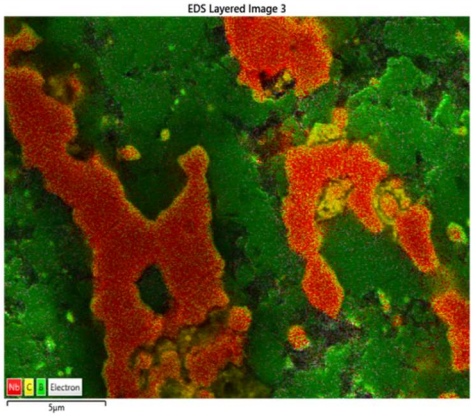

(b)

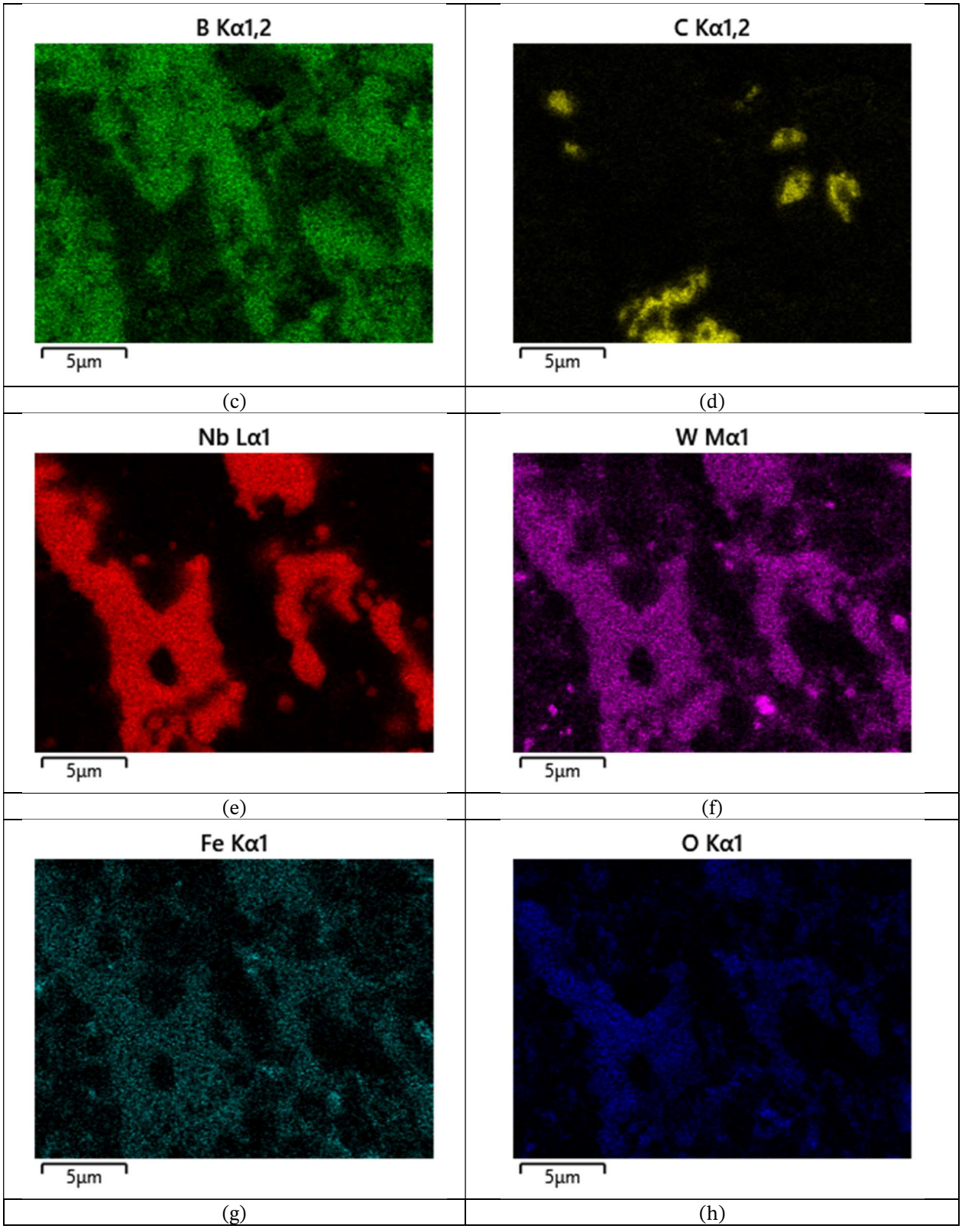

Figure 4: Region of the B_4C-Nb composite with 20% Nb mapped by EDS (a). B-rich matrix (green) containing Nb-based veins (red) (b). Regions with more intense signal for the chemical elements B (green) (c), C (yellow) (d), Nb (red) (e), W (magenta) (f), Fe (light blue) (g), O (dark blue) (h).

Table 4: Semiquantitative chemical analysis by EDS of the composite containing 20% Nb.

Chemical element	% by mass
B	53.13
C	26.62
Nb	10.38
W	2.61
Fe	1.68
O	5.58
Total	100.00%

Bulk density values obtained by mercury intrusion by Abreu [3] for the same B_4C-Nb composites used in this work are presented in Table 5. The results of Abreu [3] indicated the composite with 10% Nb as the most porous, in other words, the one with the lowest bulk density. This result is the only one in agreement with that obtained by manual DIP which showed that the highest Vv of pores was 24.87% for the composite containing 10% Nb.

Table 5: Bulk density obtained by mercury intrusion for B_4C-Nb composites [3].

Composite	Bulk density (g/cm^3)
B_4C-2% Nb	0.81
B_4C-5% Nb	0.94
B_4C-10% Nb	0.78
B_4C-20% Nb	0.88

In SEM images, it is possible to observe the heterogeneity between the different percentages of Nb using the same magnification, as shown in Fig. 5.

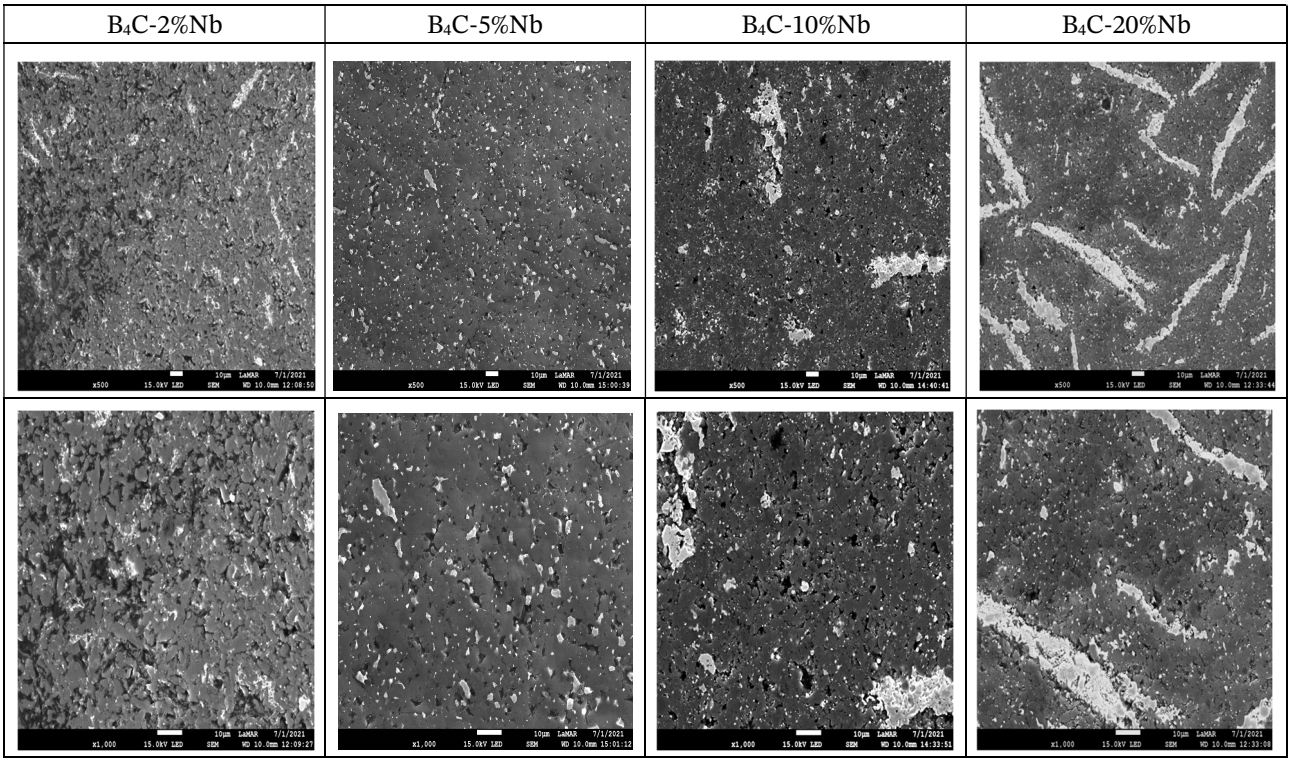

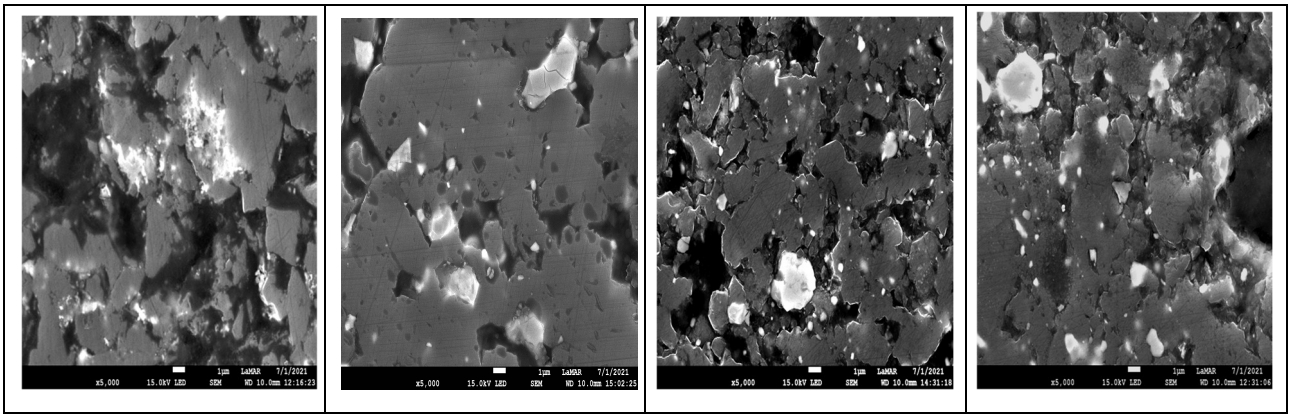

Figure 5: B_4C-Nb composite at different magnifications for 2, 5, 10, 20% Nb.

Fig. 6 shows the heterogeneity of the samples with 2% (a) and 20% (b) Nb, respectively. The images have the same 500x magnification, however there are larger regions of light tones containing Nb (b).

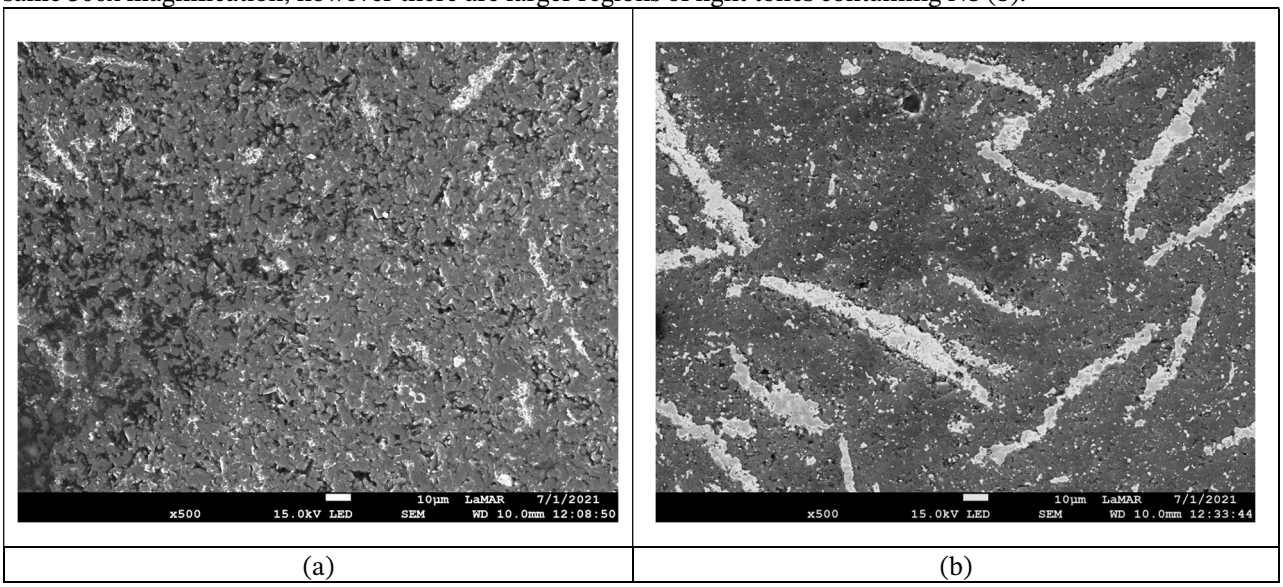

(a) (b)

Figure 6: SEM image on B_4C-Nb composites with 2% Nb (a) and 20% Nb (b) obtained 15 kV.

4 Conclusions

Obtaining adequate grinding and polishing parameters, particularly for B_4C composites containing 20% Nb, was relevant, as it allowed better conditions for the use of quantitative stereology measurements and imaging for extraction of attributes from these materials.

The SEM analyses showed that the regions of dark shades observed in the optical microscopy images were essentially pores. Thus, the use of optical microscopy as an option for applying the DIP technique can be a safe option. This safety is even greater when using manual processing rather than by stacks. The latter will only be safe when the parameters of the equipment for obtaining the images are strictly similar, generating images with similar lighting and focus parameters.

Mercury intrusion and bulk density measurements obtained in other work by Abreu [3] indicated a decreasing order for pores in groups containing 10%, 2%, 20%, and 5% Nb, different from the current work that found by the manual DIP technique that decreasing order for porosity was for composites containing 10%, 20%, 5%, and 2% Nb. These differences in results can be attributed to the heterogeneities in the presence of pores between sintered and analyzed samples from the same groups.

References

[1] A. H. Ras, F. D. Auret, and J. M. Nel, "Boron carbide coatings on diamond particles," *Diamond and Related Materials*, vol. 19, no. 11, pp. 1411–1414, 2010. Available at: https://doi.org/10.1016/j.diamond.2010.08.013.

[2] W. Ji, R. I. Todd, W. Wang, H. Wang, J. Zhang, and Z. Fu, "Transient liquid phase spark plasma sintering of B_4C-based ceramics using Ti-Al intermetallics as sintering aid," *Journal of the European Ceramic Society*, vol. 36, no. 10, pp. 2419–2426, 2016. Available at: https://doi.org/10.1016/j.jeurceramsoc.2016.03.028.

[3] G. S. Abreu, "Sinterização em alta pressão e alta temperatura (HPHT) do compósito B_4C-Nb," PhD Thesis *(in Portuguese)*, Universidade Estadual do Norte Fluminense, Campos dos Goytacazes, Brazil, 2019. Available at: https://drive.google.com/file/d/1OvXnaYxdFufq6C4kX52tApYM7VBVbjMR/view.

[4] V. C. Silva, "Medida de Porosidade em SiC Através de processamento digital de imagens," Master's Dissertation *(in Portuguese)*, Programa de Pós-Graduação em Engenharia Mecânica, Universidade do Estado do Rio de Janeiro, Rio de Janeiro, Brazil, 2015. Available at: http://www.ppgem.uerj.br/dissertacoes.html.

[5] R. C. Gonzalez and R. E. Woods, *Processamento de imagens digitais*, (in Portuguese) 1ª ed.: Editora Edgard Blucher, 2000. Available at: https://www.blucher.com.br/livro/detalhes/processamento-de-imagens-digitais-770/farmacia-e-bioquimica-111.

[6] Z. Song and Q. Y. Zhou, "Micro-scale granite permeability estimation based on digital image analysis," *Journal of Petroleum Science and Engineering*, vol. 180, no. May, pp. 176–185, 2019. Available at: https://doi.org/10.1016/j.petrol.2019.05.037.

[7] M. Uirá, "Quantificação de Defeitos por Processamento Digital de Imagens em Revestimentos obtidos por Aspersão Térmica," Master's Dissertation *(in Portuguese)*, Programa de Pós-Graduação em Engenharia Mecânica, Universidade do Estado do Rio de Janeiro, Rio de Janeiro, Brazil, 2016. Available at: http://www.ppgem.uerj.br/dissertacoes.html.

[8] H. Sun, S. Vega, and G. Tao, "Analysis of heterogeneity and permeability anisotropy in carbonate rock samples using digital rock physics," *Journal of Petroleum Science and Engineering*, vol. 156, Jul. 2017, Available at: https://doi.org/10.1016/j.petrol.2017.06.002.